Pharmaceutical Development and Technology

ISSN: (Print) (Online) Journal homepage: https://www.tandfonline.com/loi/iphd20

Tabletability and compactibility of α-lactose monohydrate powders of different particle size. I. Experimental comparison

Ann-Sofie Persson, Samaneh Pazesh & Göran Alderborn

To cite this article: Ann-Sofie Persson, Samaneh Pazesh & Göran Alderborn (2022) Tabletability and compactibility of α-lactose monohydrate powders of different particle size. I. Experimental comparison, Pharmaceutical Development and Technology, 27:3, 319-330, DOI: 10.1080/10837450.2022.2051550

To link to this article: https://doi.org/10.1080/10837450.2022.2051550

Published online: 23 Mar 2022.

PHARMACEUTICAL DEVELOPMENT AND TECHNOLOGY
2022, VOL. 27, NO. 3, 319–330
https://doi.org/10.1080/10837450.2022.2051550

Taylor & Francis
Taylor & Francis Group

RESEARCH ARTICLE

OPEN ACCESS Check for updates

Tabletability and compactibility of α-lactose monohydrate powders of different particle size. I. Experimental comparison

Ann-Sofie Persson[a], Samaneh Pazesh[a,b] and Göran Alderborn[a]

[a]Department of Pharmaceutical Biosciences, Uppsala University, Uppsala, Sweden; [b]Oasmia Pharmaceutical AB, Uppsala, Sweden

ABSTRACT

In this paper, two types of parameters representing tabletability and compactibility profiles of a series of α-lactose monohydrate powders, ranging in particle size from approximately 3.5 to 203 μm, are derived and compared. By approximating the tabletability profiles using a three-stage model and the compactibility profiles using the Ryshkewitch–Duckworth equation, two compaction rate parameters and two compaction endpoint parameters were derived. The original median particle diameter had generally a strong effect on the tablet tensile strength and hence the tabletability and compactibility profiles. The experimental profiles were well approximated by the models used, and the compaction parameters were regarded as representative of the experimental profiles. The compaction endpoint parameters increased with decreased particle size and were controlled by the same structural feature as the compacts. The tabletability rate parameter also increased with decreased particle size and correlated well with the tabletability endpoint parameter. The compactibility rate parameter tended to increase with decreased particle size, but the effect was limited; moreover, no general correlation was obtained with the compactibility endpoint parameter. It is concluded that compactibility and tabletability parameters collectively provide a concentrated description of the compaction properties of a powder.

ARTICLE HISTORY
Received 20 December 2021
Revised 4 March 2022
Accepted 7 March 2022

KEYWORDS
Compactibility; tabletability; crystalline lactose; particle size; Ryshkewitch plot; three-stage model

1. Introduction

Tablets are typically formed by confined powder compression, i.e. the transformation of a powder into a coherent tablet by the application of pressure. This compaction process involves two stages; the reduction in volume of the powder, which will decrease the separation distance between particle surfaces, followed by the formation of inter-particle bonds. Compression is defined as the reduction in volume of the powder and the term powder compressibility refers to the propensity of a powder to reduce in volume, a property typically quantified by parameters derived from compression equations. The ability of a powder to form a tablet is obviously critical for the success of a tableting operation and a fundamental quality attribute of a tablet is its resistance towards breakage, often assessed by the tablet tensile strength. The tablet tensile strength is affected by a series of particle properties, such as their size (Alderborn and Nyström 1982; Adolfsson and Nyström 1996), shape (Alderborn et al. 1988) and surface energy (Fichtner et al. 2008). It is, for example, frequently reported that small particles form tablets of higher tablet tensile strength compared to large particles (Butcher et al. 1974; Vromans, Deboer, Bolhuis, Lerk, Kussendrager 1985; Cabiscol et al. 2020). Furthermore, particle size can affect the mechanical response during compression since small particles typically require a higher applied pressure for plastic deformation and are less prone to fragment than large particles (Hersey et al. 1973).

In order to characterise the ability of a powder to form a tablet, the tensile strength is often related to the solid fraction of the tablet (Wu et al. 2005, 2006), i.e. the relationship between two tablet properties is used to describe a powder property. An alternative approach to describe the cohering ability of a powder is the relationship between tablet tensile strength and the compression force or pressure applied to the powder, i.e. the relationship between a tablet property and a process parameter. It has been common in the literature to refer to these two types of relationships, i.e. tensile strength – porosity and tensile strength – compaction pressure, as the compactibility and the tabletability of a powder, respectively (Tye et al. 2005). However, since both tensile strength and solid fraction of a tablet depend on the applied pressure, compactibility and tabletability have some interrelationship.

A series of equations attempting to describe relationships between tensile strength – porosity and tensile strength – compaction pressures, respectively, have been proposed (Sonnergaard, 2006). The dominating compactibility expression used in the pharmaceutical literature is the Ryshkewitch–Duckworth equation (Duckworth 1953; Ryshkewitch 1953). The expression contains two parameters: the first describing the evolution in tablet tensile strength with reduced porosity and the second the tablet tensile strength at zero porosity. Theoretically, the tensile strength at zero porosity corresponds to the strength of the material. In practice, the parameter is obtained by extrapolation of a plot of the tensile strength of tablets as a function of their porosity, and there does not appear to be a unanimous agreement of the physical meaning of this extrapolated strength (Adolfsson and Nyström 1996; Steendam and Lerk 1998). Regarding the tabletability, several

CONTACT Ann-Sofie Persson ann-sofie.persson@farmbio.uu.se Department of Pharmaceutical Biosciences, Uppsala University, Box 591, SE-751 24 Uppsala, Sweden

mathematical relationships have been proposed, including both linear (Newton et al. 1971; Sonnergaard, 2006; Ilic et al. 2009) and power expressions (Kuentz and Leuenberger 2000), but no relationship has gained a similar recognition as the corresponding Ryshkewitch–Duckworth equation. Some of the tabletability expressions focus primarily on a limited pressure range and not on the complete strength–pressure profile. A complete strength–pressure profile is typically sigmoidal (Rees and Rue 1978; Sonnergaard, 2006), with a tablet tensile strength plateau that requires the application of high compaction pressures to be observed experimentally (Adolfsson and Nyström 1996; Tye et al. 2005; Persson and Alderborn 2018). This tablet tensile strength plateau is typically not associated with a tablet of zero porosity, although such an observation has been reported (Adolfsson and Nyström 1996). Sonnergaard (2006) proposed that a simple linear expression, in an appropriate way, describes relationships between a specific crushing strength and the compaction pressure within the region during which the tensile strength increases with applied pressure. The gradient of the line can hence be used as a descriptor of the powder tabletability. As an extension of this reasoning, an approach to methodise the relationship between tablet tensile strength and compaction pressure has been presented (Alderborn 2003). This model approximates the sigmoidal strength–pressure relationship into three regions, where the middle region, in which the tensile strength increases with applied pressure, is assumed to be linear until the maximum achievable tensile strength is reached. The model has also been successfully used to predict the tabletability of a series of powders (Persson and Alderborn 2018). In accordance with this approach, two tabletability parameters can be determined which principally corresponds to the parameters of the Ryshkewitch–Duckworth relationship, i.e. a gradient showing the evolution in tensile strength with increased pressure and an endpoint representing the maximum tensile strength achieved. These parameters represent indications of the complete tabletability and compactibility profiles. Due to the interrelation between compactibility and tabletability, the correspondence between the parameters deserves to be further investigated, as well as their physical significance.

Hence, the objective of this paper was to compare the tabletability and the compactibility of some powders using parameters derived from strength-pressure and strength–porosity relationships. In order to calculate such parameters, the same principal type of handling of the relationships was done, i.e. two parameters are calculated for each relationship, one indicating the evolution in tensile strength (rate parameter) and one the maximum tensile strength (endpoint parameter). To our knowledge, a similar type of comparison of compactibility and tabletability of powders has not previously been reported in the literature. Since the particle size is known to influence the cohering ability of a powder, a series α-lactose monohydrate powders, ranging in median particle size (d_{50}) from approximately 3.5 to 203 μm, as measured by laser diffractometry, was selected as model materials. With this approach, a comparison can be made between powders with different tablet forming abilities but of the same crystal structure and surface energy i.e. material properties that may affect both the inter-particulate bonding and the fracturing properties of a compact.

2. Materials and methods

2.1. Materials

Seven qualities of crystalline α-lactose monohydrate powder were used. Pharmatose® 80 M (CL80), Pharmatose® 130 M (CL130), Lactohale® LH201 (LH201), Lactohale® LH230 (LH230), Lactohale® LH300 (LH300) and Lactochem® Microfine (LCMF) were obtained as generous gifts from DFE Pharma, The Netherlands. Pharmatose® 200M (CL200) was purchased from DMV, The Netherlands. Magnesium stearate (Sigma-Aldrich, Sweden) was used as a lubricant. Ethanol 95% w/w (Solveco, Sweden) and 2-propanol (VWR, Sweden) were used as dispersion media. Prior to further characterisation, the powders were stored in a humidity-controlled laboratory at 33 ± 3% relative humidity and at room temperature for a minimum of seven days. The unsettled bulk density, the compression and the compaction experiments subsequently described were performed in the same humidity-controlled laboratory using the same conditions.

2.2. Determination of particle diameter and particle and powder density

The particle size distribution for all lactose powders was determined by laser diffraction (Coulter LS230, small volume module plus, Coulter Corporation, Miami, United States) using a particle refractive index of 1.533, a dispersant refractive index of 1.378 and an imaginary refractive index of 0.1. For all particle diameter measurements, a suspension of about 100 mg lactose were prepared using 5 ml of 2-propanol as dispersion vehicle. Prior to the analysis, the suspensions were sonicated for 10 min in a water bath (Ultrasonic Cleaner Branson, B5210E-MT, Branson Ultrasonic Company, Danbury, United States) at a frequency of 47 kHz ± 6% for all powders, except CL80 and CL130. The latter powders were excluded to avoid particle fragmentation during preparation.

The sample cell of the diffractometer was filled with 2-propanol which was stirred with a rotating stirring bar and an appropriate volume of the suspension was then added and the measurement performed. The particle diameter was calculated according to the Fraunhofer theory. The median particle diameter (d_{50}) of a volume distribution was determined and reported median particle diameters are the average of one (with 10 runs) or two (with five runs) independent measurements.

The apparent particle density (ρ_{app}, number of independent measurements, $n = 3$) was measured by helium displacement pycnometry (Micromeritics AccuPyc II 1340, Micromeritics Instrument Corp., Norcross, United States), with the powder held in a 10 cm^3 sample chamber. The measurements were performed with run precision mode, and an average of a minimum five cycles was used for each independent measurement.

The poured (unsettled) powder bulk density (ρ_{bulk}, $n = 3$) was measured using a 10 ml glass cylinder of 11.1 mm in diameter (similar to the diameter of the die used during powder compression described in Section 2.3. below). The cylinder was filled with powder by gentle pouring through a funnel, and the powder weight was recorded thereafter.

2.3. Powder compression

Approximately 320–400 mg powder was uniaxially compressed ($n = 5$) up to 300 MPa in a materials tester (Zwick Z100, Zwick/Roell GmbH & Co, Germany) equipped with flat-faced punches with a diameter of 11.3 mm. The lower punch was stationary and the upper punch moved at a rate of 10 mm/min both during compression and decompression. Prior to compression, the die and the punch faces were lubricated using a 1% (w/w) magnesium stearate suspension in ethanol. The elastic system deformation was measured to 0.4 μm/MPa as described earlier

(Nordström et al. 2008) and was accounted for in the calculation of tablet height in the compression analysis.

Compression profiles were derived in accordance with the Kawakita (Kawakita and Lüdde 1971) and the Heckel (1961) equations, as reported earlier (Persson and Alderborn 2018). The engineering strain in-die was calculated using the initial powder bed height assessed from in-die powder weight and ρ_{bulk}. The linear form of the Kawakita equation was used for determinations of the Kawakita a and b^{-1} parameters, using linear regression ($R^2 > 0.999$) in the pressure interval 20–290 MPa. In addition, the *ab*-index (ab_I) was calculated as an indication of the particle rearrangement propensity (Nordström et al. 2009). The Heckel in-die yield pressure (P_y) was calculated as the reciprocal of the slope of the linear part of the Heckel plot, determined by linear regression ($R^2 > 0.999$) as described earlier (Mahmoodi et al. 2013). From the decompression stage, the in-die elastic recovery (ER_{in-die}) was derived, as described earlier (Persson et al. 2018).

2.4. Powder compaction

Powder was compacted in an eccentric tablet press (Korsch EK0, Germany) equipped with either flat-faced circular punches with a diameter of 11.3 mm (for pressures up to 300 MPa) or 5.65 mm (for pressures from 300 to 1200 MPa). A constant minimum punch separation distance was used during powder compaction, controlled by using metal stubs of 3 mm (for 11.3 mm punches) or 2 mm (for 5.65 mm punches) height. The powders were compacted in a pressure range between approximately 20 and 1200 MPa ($n = 5$ at each applied pressure), and the compaction pressure was controlled by the amount of powder filled into the die. It should be noted that the pressure range used varied between each individual lactose quality. The die and punches were lubricated prior to compaction in the same way as described in Section 2.3.

After tablet ejection, the tablet height and diameter were measured using a height gauge (Litematic VL 50 A, Mitutoyo, Japan). Thereafter, the force needed to fracture the tablets while compressed diametrically in a tablet hardness tester (Holland C50, UK, with a rate of 1 mm/min, or PharmaTest PTB311E, Germany, with a linear force increase rate of 20 N/s) was measured. The tablet tensile strength (σ_t) was subsequently calculated according to Fell and Newton (Fell and Newton 1970).

2.5. Imaging

Images of discrete particles and fracture surfaces of compacts were obtained by scanning electron microscopy (SEM) at an accelerating voltage of 2 kV using a Leo (Zeiss), 1550 Schottky (Germany) microscope. Prior to the scanning, the samples, i.e. the particles or the compact fragments, were sputtered with Au/Pd in a sputter coater (Polaron, Quorum Technologies Ltd., Newhaven, UK). The compact fragments used for imaging were prepared by fracturing tablets compacted at 300 MPa (Section 2.3) by diametrical compression in the tablet hardness tester (PharmaTest, PTB311E, Hainburg, Germany) as described in Section 2.4 but without recording the fracture force.

2.6. Tabletability analysis

The strength–pressure relationships, i.e. the tabletability, were approximated for all materials using the three-stage compaction model (Alderborn 2003), and the slope of the linear region (k_c; Pazesh et al. 2019) and the tablet tensile strength at the strength-pressure plateau (Persson and Alderborn 2018), hereinafter denoted as the maximum tensile strength ($\sigma_{t,max}$), were the derived tabletability parameters. k_c was calculated using linear regression ($R^2 > 0.975$) of the pressure range up to 700 MPa. For CL80, CL130, CL200 and LH201, the strength–pressure plateaus were considered to range over the four highest compaction pressures, and $\sigma_{t,max}$ was determined as the average σ_t of the strength–pressure plateaus. For the three other lactose powders, a reduction in σ_t occurred at the highest compaction pressures used, i.e. stable plateaus were not obtained, and the $\sigma_{t,max}$ for LH230 and LCMF was determined as the average of the four highest σ_t recorded and for LH300 as the average of the two highest σ_t values recorded.

2.7. Compactibility analysis

The Ryshkewitch–Duckworth equation (Duckworth 1953; Ryshkewitch 1953) was used to analyse the relationship between σ_t and tablet porosity (ε), i.e. the compactibility, as described recently (Pazesh et al. 2019). ε was calculated as $1-(\rho_{tab}/\rho_{app})$, where ρ_{tab} is the tablet density determined from the tablet mass and dimensions. Linear regression was applied for calculations of the slope and the intercept to be used as the bonding capacity factor (k_R) and the tablet tensile strength at zero porosity (σ_0), respectively. Two sets of compactibilty parameters were derived: the first set (denoted a) was calculated using the complete porosity range ($R^2 > 0.969$), whereas the second set (denoted b) was calculated using the porosity range for applied pressures up to 700 MPa ($R^2 > 0.977$), i.e. the corresponding porosity range as used for determination of k_c as described in Section 2.6.

2.8. Tablet strength-particle size relationship

As a means to describe the relationship between the average tablet tensile strength and the original particle diameter, the Orowan equation (Orowan 1949), as modified by Knudsen (1959), was used, i.e.

$$\ln\ \sigma_t = \ln\ \sigma_K - k_K\ \ln\ d_{50}, \quad (1)$$

where k_K and σ_K are constants calculated as the slope and the intercept, respectively, using linear regression ($R^2 > 0.897$). The relationship was applied to tablets formed at three compaction pressures of the linear region of the tabletability relationship of approximately 100, 300 and 500 MPa (94.5 MPa ± 6.65 standard deviation (SD), 287 MPa ± 7.99 SD and 522 MPa ± 16.9 SD) and two compaction pressures of the plateau region of the tabletability relationship of approximately 800 and 1000 MPa (808 MPa ± 35.2 SD and 1031 MPa ± 30.3 SD). Finally, the extrapolated tablet tensile strength of the second compactibility set, i.e. σ_{0_b}, (see Section 2.7) was also used.

2.9. Statistical analysis

One-way analysis of variance (ANOVA) followed by Tukey *post hoc* test was performed where applicable. The significance level was set to 95%; thus, $p < 0.05$ was regarded as statistically significant.

3. Results

3.1. Particle and powder properties

The median original particle diameter (d_{50}) of the studied grades of lactose ranged from about 3.5 μm for LH300 to about 203 μm for CL80 (Table 1), and LH300 and LCMF had approximately the

same d_{50}. The particle size distributions of the powders appeared to be generally relatively broad (Figure 1), and the span ranged from 1.4 to 2.6 (Table 1). For LCMF and LH300, sub-micron sized particles adhered to the surface of the larger particles. The single particles of all lactose qualities had a similar geometric shape, irrespective of particle size (Figure 1); a shape typical of crystalline lactose particles and often denoted as a tomahawk shape.

The densities of the powders were determined using helium pycnometry. It has been reported that using this method to measure densities of hydrates (Sun 2004) can be flawed due to the loss of crystal water during the measurement. However, it is also reported that α-lactose monohydrate is stable and does not lose water during measurement (Chang et al. 2019). All lactose powders had nearly the same apparent particle density (ρ_{app}, Table 1), ranging between 1.54 and 1.55 g/cm^3 and similar to earlier reported values for α-lactose monohydrate powders (Pazesh et al. 2018).

The unsettled bulk density (ρ_{bulk}) increased (Table 1) with increased particle size as expected (Castellanos 2005). The two powders with similar d_{50}, i.e. LH300 and LCMF, had the same ρ_{bulk} ($p > 0.05$). Since the particle shape was similar for all powders, the change in ρ_{bulk} was dictated predominantly by the differences in particle size.

3.2. Compression properties

It is well known that the type of lactose used in this study fragments during powder compression, and the size distribution of the particles forming the compact, may thus be different compared to the original particles. SEM images of fracture surfaces of compacts (Figure 2) showed that roughness of the fracture surfaces decreased with reduced particle size. For compacts formed of the larger original particle sizes, e.g. CL80 and CL130 (upper row in Figure 2), large discrete particles could be identified, and small cracks in the particles could also be observed. For compacts formed of the three powders with smallest original particle size, i.e. LH230, LCMF and LH300 (lower row in Figure 2), the fracture surfaces were smooth, and it was difficult to observe discrete particles or cracks. It was generally difficult to judge if the fracture occurred around or across the original particles. The SEM images of the tablet fracture surfaces show that tablets formed of larger original particles consisted of larger particles than tablets formed of smaller original particles. The SEM images also indicate that the inter-particulate tablet pore structure became more closed with decreased particle size. Thus, the tablet microstructure depended on the original particle size, and a difference in original particle size will not be eliminated by particle fragmentation during compression.

Table 1. Particle and powder characteristics. Relative standard deviations are given in parentheses.

	d_{50} (μm)[a]	Span	ρ_{app} (g/cm^3)[b]	ρ_{bulk} (g/cm^3)[c]
CL80	203.4	1.6	1.540 (<0.01)	0.78 (0.01)
CL130	75.2	2.0	1.541 (<0.01)	0.62 (0.02)
CL200	27.4**	2.2**	1.537 (<0.01)*	0.52 (0.01)*
LH201	15.7	2.6	1.547 (<0.01)	0.42 (0.01)
LH230	8.12	2.6	1.551 (<0.01)	0.32 (0.02)
LCMF	3.86	2.0	1.552 (<0.01)	0.26 (<0.01)
LH300	3.46**	1.4**	1.547 (<0.01)	0.27 (0.01)

* Obtained from Persson and Alderborn (2018).
**Obtained from Pazesh et al. (2018).
[a]Median particle diameter.
[b]Apparent particle density ($n = 3$).
[c]Unsettled bulk density ($n = 3$).

The compression process was also strongly affected by the original particle size, and the Kawakita a and b^{-1} parameters and the Heckel yield pressure (P_y) varied significantly ($p < 0.05$) between the powders (Table 2). The Kawakita a parameter increased and the Kawakita b^{-1} parameter decreased with reduced particle size, i.e. decreasing original particle size gave powders of increasing compressibility. The combination of the Kawakita parameters into an index, i.e. the ab_l-index, gave index values which were dependent on the original particle size. The powders having a particle size larger than about 27 μm, i.e. CL80 and CL130, had an ab_l-index smaller than 0.1, while the other had values above 0.1. Thus, only the two powders with the largest original particles showed limited particle rearrangement (Nordström et al. 2009). The increased compressibility with reduced particle size could thus be explained by an increased degree of particle rearrangement during compression.

The P_y increased with decreased particle size (Table 2), reflecting an increased particle plastic stiffness with decreased particle size. This is in accordance with earlier experiences (Pazesh et al. 2018) and typically explained by a reduction in the number of crystal defects with a reduced particle size, causing a higher resistance to particle deformation. In Figure 3, the relationship between the original median particle diameter and the P_y is shown. For the coarser grades of lactose powders (CL80, CL130 and CL200), only a small reduction in P_y with a decreased particle diameter was obtained, but for the finer grades (LH201, LH230, LCMF and LH300), P_y increased markedly with reduced particle

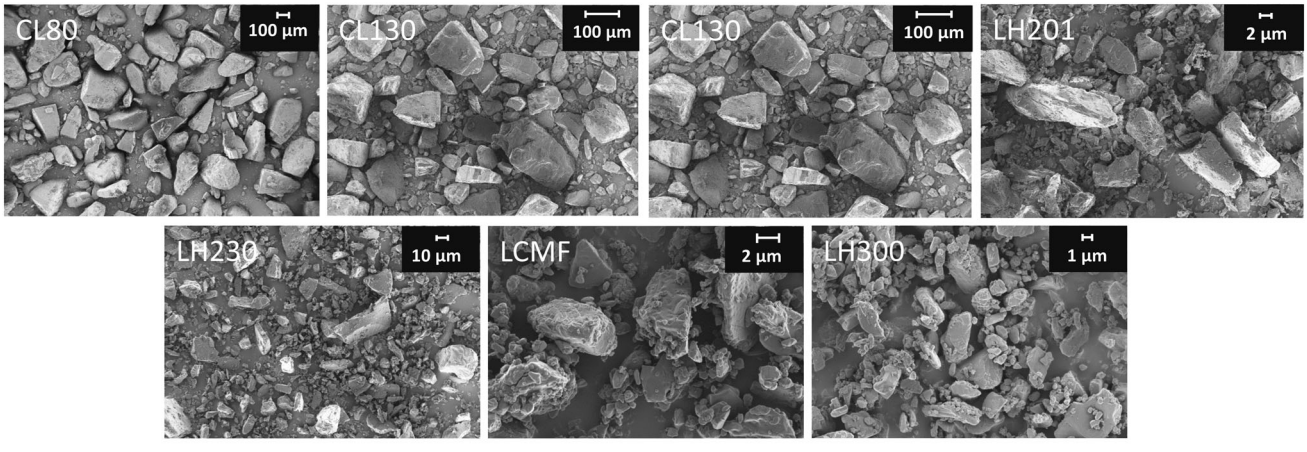

Figure 1. Scanning electron micrographs of the studied lactose powders. Note the varying scales of the images.

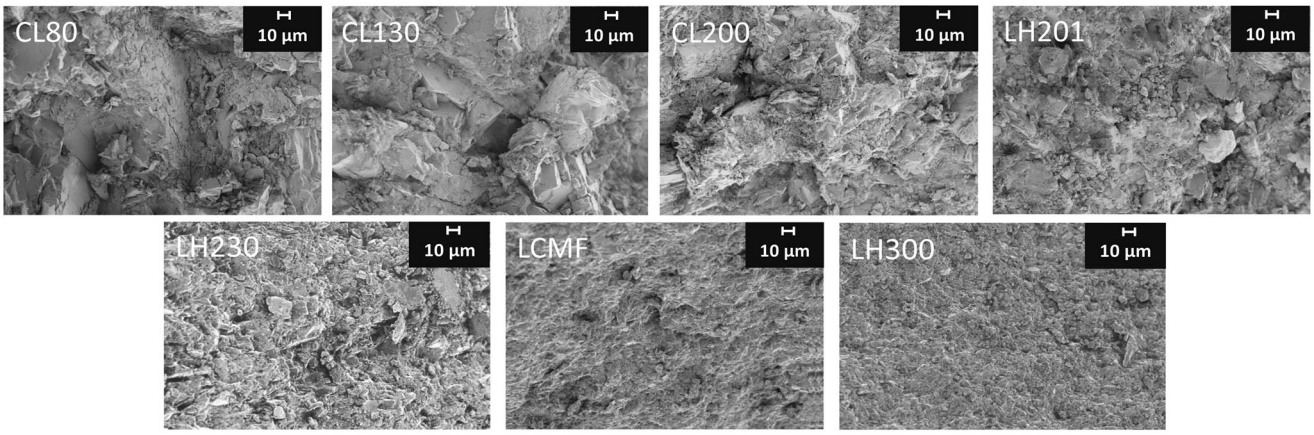

Figure 2. Scanning electron microscopy images from compact fracture surfaces.

Table 2. Compression characteristics. Relative standard deviations are given in parentheses.

	a (–)[a]	b^{-1} (MPa)[b]	ab_l (–)[c]	P_y (MPa)[d]	ER_{in-die} (%)[e]
CL80	0.493 (0.001)	11.9 (0.002)	0.04 (0.002)	147.7 (0.009)	3.41 (0.005)
CL130	0.588 (0.001)	7.06 (0.011)	0.08 (0.012)	159.3 (0.011)	3.38 (0.021)
CL200	0.663 (<0.001)	5.79 (0.004)	0.11 (0.004)	164.3 (0.010)	3.12 (0.020)
LH201	0.719 (<0.001)	4.52 (0.001)	0.16 (0.001)	176.9 (0.003)	3.16 (0.005)
LH230	0.781 (<0.001)	3.68 (0.002)	0.21 (0.002)	190.7 (0.004)	2.78 (0.004)
LCMF	0.825 (<0.001)	2.90 (0.002)	0.28 (0.002)	206.8 (0.009)	2.78 (0.007)
LH300	0.816 (<0.001)	3.29 (0.001)	0.25 (0.002)	202.1 (0.006)	3.03 (0.006)

[a]Kawakita parameter ($n = 5$).
[b]Kawakita parameter ($n = 5$).
[c]Particle rearrangement index ($n = 5$).
[d]Heckel yield pressure ($n = 5$).
[e]In-die elastic recovery ($n = 5$).

diameter. Thus, an abrupt change in particle plastic stiffness – particle diameter profile was obtained at a medium particle diameter below 27 µm, indicated by the dotted vertical line in Figure 3. Below this particle size, the P_y became strongly dependent on the particle diameter. Thus, the particle plastic stiffness, as assessed by the Heckel relationship, changed markedly at a critical particle size of about 20–30 µm.

One may notice that the LCMF and LH300 powders had nearly the same original particle size (d_{50}, Table 1), but the derived compression parameters differed significantly ($p < 0.05$) between these powders. LCMF had a higher a parameter and P_y and a lower b^{-1} than LH300 (Table 2). However, the absolute differences were small, and the powders must be described as having similar compression behaviour.

There was a relatively small but significant variation ($p < 0.05$) in the in-die elastic recovery of the tablets (Table 2). The ER_{in-die} were ranked in the following order from high to low, CL80 = CL130 > CL200 = LH201 > LH300 > LH230 = LCMF, i.e. a weak trend of reduced ER_{in-die} with decreased particle size was obtained.

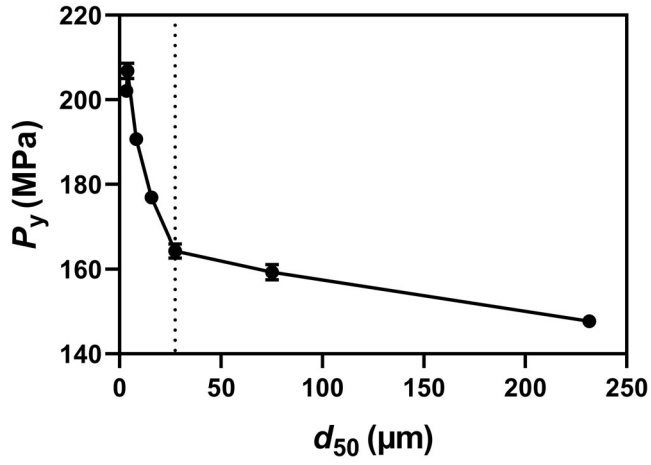

Figure 3. Heckel yield pressure (P_y) as a function of original particle diameter (d_{50}). The vertical dashed line represents the brittle-ductile transition for α-lactose monohydrate (Roberts and Rowe 1987). The error bars display the standard deviations.

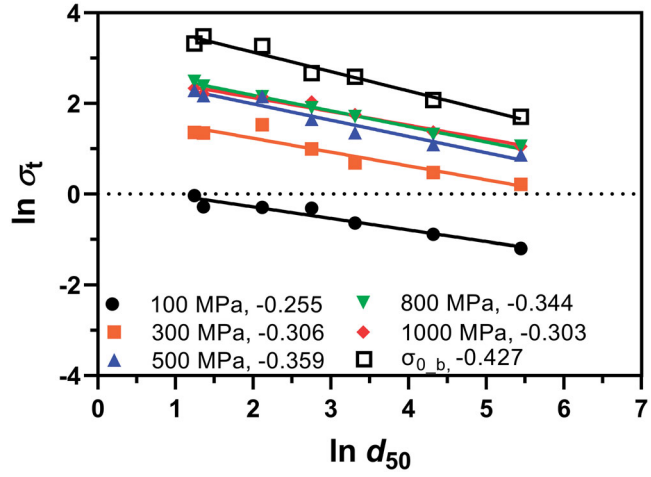

Figure 4. Natural logarithm of tablet tensile strength (ln σ_t) as a function of natural logarithm of original particle diameter (ln d_{50}).

3.3. Compaction properties

3.3.1. Tablet strength – particle diameter relationship

The effect of particle size on the ability of a powder to cohere into a tablet is often described by the relationship between the original particle diameter and the tensile strength of tablets formed at a constant compaction pressure. For the lactose powders used in this study, the tablet tensile strength increased with a decreased original median particle diameter, as shown by the linear relationships between ln σ_t and ln d_{50} ($R^2 > 0.897$) for the five selected pressures (Figure 4). The increased compaction pressure shifted the lines parallel to each other until the highest compaction pressures, at which the relationships coincided. Hence, the slope (k_K) of the relationship was independent of the compaction pressure (as shown by the numbers in Figure 4).

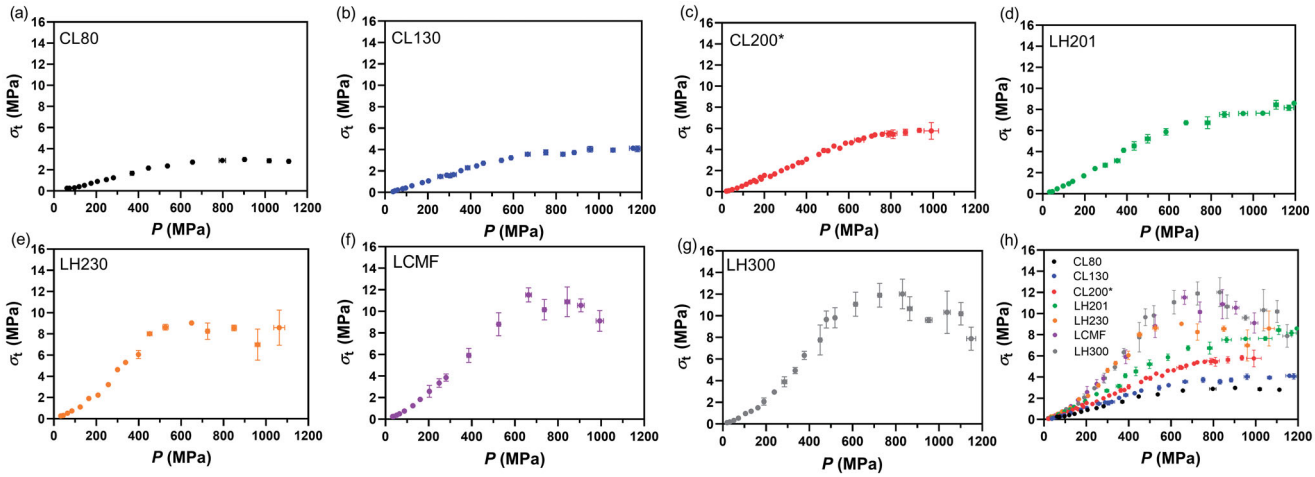

Figure 5. Tabletability relationships i.e. tablet tensile strength (σ_t) as a function of compaction pressure (P) for the single α-lactose monohydrate powders (a-g) and a comparison between all powders (h). The error bars display the standard deviations. *Data obtained from Persson and Alderborn (2018).

Table 3. Characteristics of tabletability and compactibility profiles. Relative standard deviations are given in parentheses.

	Tabletability		Compactibility			
	k_c x 10^{-3} (–)[a]	$\sigma_{t,max}$ (MPa)[b]	σ_{0_a} (MPa)[c]	k_{R_a} (–)[d]	σ_{0_b} (MPa)[e]	k_{R_b} (–)[f]
CL80	4.53	2.88 (0.024)	5.82	14.33	5.51	14.02
CL130	5.75	4.04 (0.019)	8.19	17.44	7.97	17.29
CL200	7.99	5.67 (0.029)	13.1	18.42	13.7	18.53
LH201	10.6	8.21 (0.051)	14.3	15.33	14.4	15.39
LH230	16.4	8.62 (0.037)	20.0	12.77	26.3	13.93
LCMF	18.0	10.8 (0.054)	26.5	13.86	32.6	14.67
LH300	19.9	12.0 (0.008)	22.6	13.51	27.8	14.33

[a]Slope of the linear pressure region.
[b]Average maximal tablet tensile strength.
[c]Extrapolated tensile strength, derived using the complete porosity range.
[d]Bonding capacity factor, derived using the complete porosity range.
[e]Extrapolated tensile strength, derived using porosities generated at applied pressures <700 MPa.
[f]Bonding capacity factor, derived using porosities generated at applied pressures <700 MPa.

3.3.2. Tabletability

The particle size strongly influenced the tabletability profiles (Figure 5). The four powders with the largest original particle diameter (CL80, CL130, CL200 and LH201) showed an evolution in tablet strength with compaction pressure that was nearly linear until a relatively sharp bending of the profiles was reached, and a constant tablet tensile strength with increased compaction pressure was obtained (Figure 5(a–d)), i.e. a stable tablet tensile strength plateau. Thus, the tabletability of these lactose powders could generally be well approximated using the three-stage compaction model (Alderborn 2003). Both the rate of increase in strength with pressure and the plateau tablet strength increased markedly with decreased particle size. For the three powders with the smallest original particle diameter, i.e. below ~10 μm (LH230, LCMF and LH300), the tabletability profiles were more clearly sigmoidal, with an initial slightly bended increase in σ_t with pressure followed by a linear region, which finally levelled off to a maximum tablet strength (Figure 5(e–g)). Similar sigmoidal tabletability profiles have also been reported for other materials (Rees and Rue 1978; Sonnergaard, 2006). Moreover, for these powders, a reduced d_{50} increased the rate of strength increase with pressure until the maximum tablet strength was obtained.

The finest powders did not show a constant tablet strength at the highest compaction pressures, and a tendency to a reduction in tablet strength with increased pressure was obtained, most pronounced for LCMF and LH300 (Figure 5(f,g)). Thus, for the finest powders, stable plateaus comparable to the coarser powders were not obtained, and the spread in tablet tensile strength was higher at the highest compaction pressures.

Regardless of the differences in the character of the tabletability profiles, they were all approximated as a three-stage process, and two tabletability parameters were accordingly calculated, i.e. the slope of the linear region (k_c) and the maximal tablet tensile strength ($\sigma_{t,max}$). Both k_c and $\sigma_{t,max}$ increased gradually with decreased particle diameter (Table 3), except for LH201 and LH230, which had similar values of $\sigma_{t,max}$. For both parameters, non-linear relationships to the original particle diameter were obtained (Figure 7), similar to the relationship between P_y and particle diameter (Figure 3). The range of compaction pressures, within which the tablet tensile strength increased with compaction pressure until $\sigma_{t,max}$ was reached, varied between approximately 550 MPa and 800 MPa. Nevertheless, the two tabletability parameters were related nearly linear to each other (Figure 8(a)).

3.3.3. Compactibility

The compactibility profiles were plotted according to the Ryshkewitch-Duckworth equation (Figure 6). The lowest tablet porosity obtained was similar for all powders, about 4–6% (as indicated by the dotted vertical lines in Figure 6). However, the range of tablet porosities obtained was influenced by particle size, i.e. the tablet porosity range was narrower for the coarser powders (Figure 6(a–d)) than for the finer powders (Figure 6(e–g)). The Ryshkewitch–Duckworth equation gave satisfactory approximations of the compactibility of the powders in accordance with earlier studies on α-lactose monohydrate powders (Tye et al. 2005; Wu et al. 2006; Pazesh et al. 2019). However, some of the lactose powders gave slightly bended relationships at the highest tablet porosities, with a somewhat higher rate of change in ln σ_t with porosity. Moreover, some of the profiles levelled off at the lowest tablet porosities, which corresponded to the part of the tabletability profiles at which a strength plateau was obtained or at which the tablet strength decreased. A levelling off of the Ryshkewitch–Duckworth plots at low tablet porosities has also been reported earlier (Pazesh et al. 2019). Depending on the porosity range over which this levelling off occurs, it will have a more or less marked effect on the

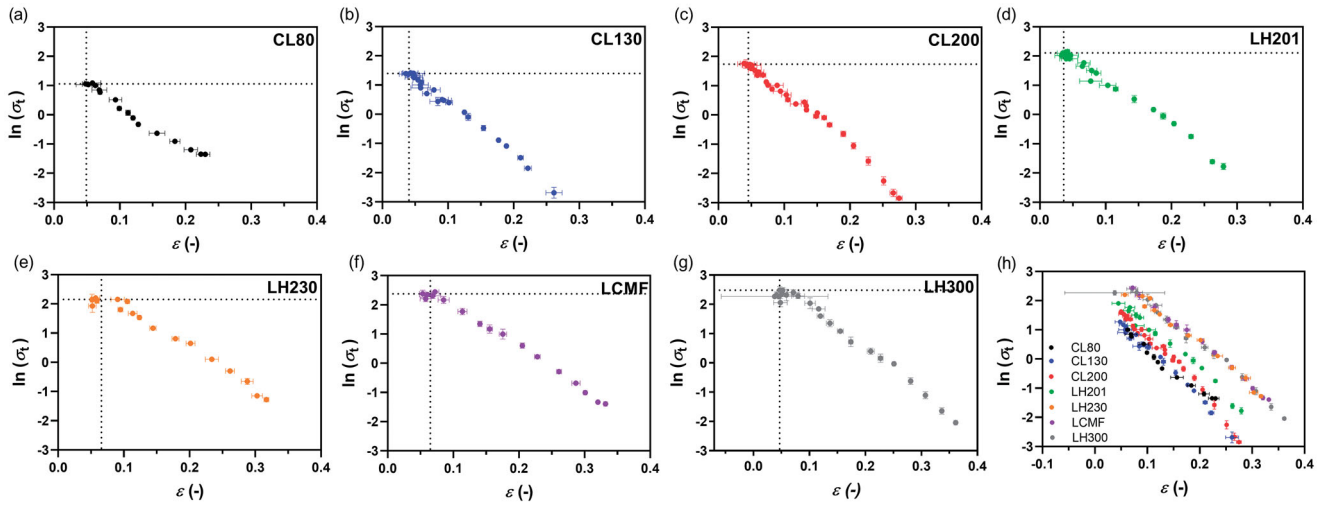

Figure 6. Compactibility relationships i.e. tablet tensile strength (σ_t) as a function of tablet porosity (ε) for the single α-lactose monohydrate powders (a–g) and a comparison between all powders using pressures <700 MPa (set b) (h). The dotted horizontal lines represent the maximum tensile strength ($\sigma_{t,max}$), and the dotted vertical lines represent the porosity at $\sigma_{t,max}$. The error bars display the standard deviations.

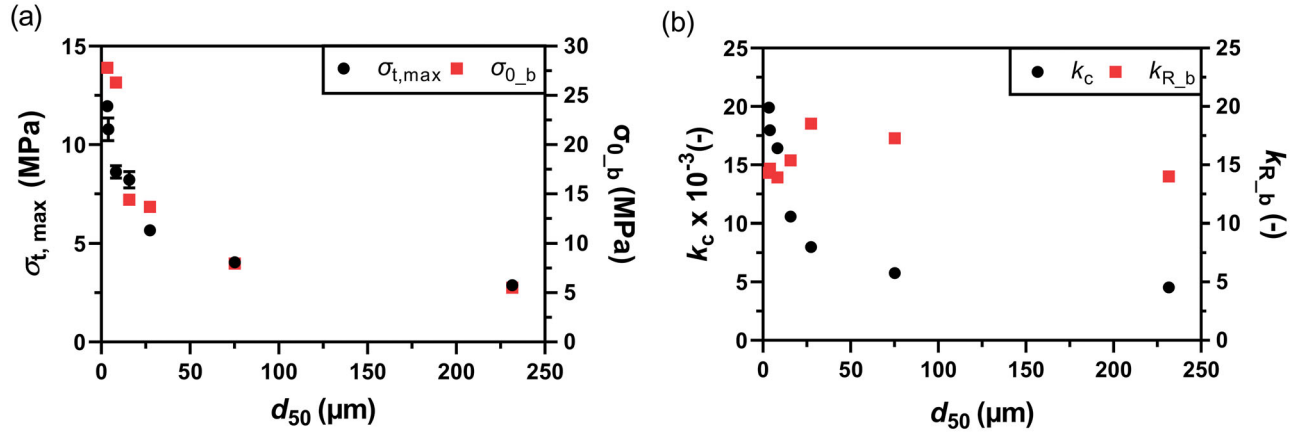

Figure 7. Tensile strength descriptors representing tabletability and compactibility as a function of original particle diameter (d_{50}). (a) tensile strength endpoints i.e. $\sigma_{t,\ max}$ and σ_{0_b} and (b) tensile strength rate parameters i.e. k_c and k_{R_b}. The error bars display the standard deviations.

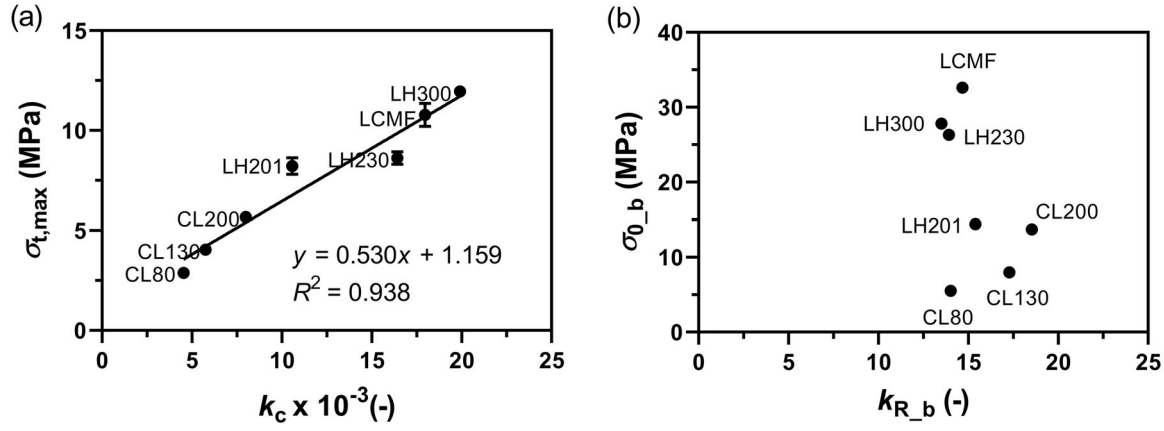

Figure 8. Relationship between endpoint and rate parameters for (a) tabletability and (b) compactibility. The solid line in (a) is the linear regression line. The error bars display the standard deviations.

Ryshkewitch–Duckworth parameters, i.e. σ_0 and k_R. Consequently, two sets (denoted a and b) of the parameters were calculated (Table 3). The first set (a) was calculated using the whole range of tablet porosities, and the second set (b) was calculated for tablet porosities obtained at applied pressures <700 MPa (Figure 6(h)).

Since the lowest porosities of the tablets achieved by the compaction were typically around 4–6%, the extrapolation down to

zero porosity gave consequently higher values of σ_0 than $\sigma_{t,\,max}$ (Table 3). For both ranges of tablet porosity used for the extrapolation (sets a and b), the σ_0-values for the coarser grades of powders were generally approximately a factor of two larger than the $\sigma_{t,\,max}$-values, while for the finer grades, factors of about 2–3 were obtained depending on the porosity range used. Thus, although the extrapolation was done over a relatively limited range of tablet porosities, markedly higher values of σ_0 than of $\sigma_{t,\,max}$ were obtained.

The σ_0 (Table 3) was markedly influenced by particle size and increased steadily but non-linearly with decreased d_{50} (Figure 7(a)), except for LH300 which had a similar d_{50} as LCMF (Table 1) but gave a slightly lower σ_0 than LCMF. In analogy with the relationships between original particle diameter and tablet tensile strength, the relationship between ln σ_{0_b} vs ln d_{50} was also approximately linear and shifted in parallel to the ln σ_t vs ln d_{50} relationships and with similar slope as the other relationships (Figure 4).

A similar monotonous change as for k_c, $\sigma_{t,\,max}$ and σ_0 as a function of d_{50} was not obtained for k_R (Table 3). For CL80, CL130 and CL200, the k_R increased with decreased particle size but, as the particle size decreased further, the k_R was reduced slightly (LH201) and became approximately constant for the three finest powders (for powders with $d_{50} < 10\,\mu m$; Table 3). For these finest powders, the k_R was lower than for CL80, despite the much higher σ_0. Thus, k_R increased until a critical particle size was reached and thereafter, lower and approximately similar values of k_R were obtained (Figure 7(b)).

4. Discussion

Tabletability and compactibility profiles are commonly used as indications of the ability of a powder to form a tablet. In this study, these two approaches are compared by the use of parameters derived from each type of profiles, i.e. two parameters representing endpoints of the profiles and two representing rates of change. Since it is generally known that the original particle size of powders will affect their ability to form tablets, a series of powders of varying original particle diameters were used in the comparison.

The transformation of a powder into a compact is fundamentally an inter-particulate bond formation process and the position taken in the discussion of the compaction data in this paper is a bond summation concept, i.e. the tensile strength of the compact equates the sum of the bonding forces acting between particles over the fracture area (alternatively expressed as the product between the bonding area per cross-sectional area of tablet and the bond strength). Since all powders used were of the same substance and the same solid state, i.e. crystalline α-lactose monohydrate, it can be expected that they have similar chemical composition and surface energy and hence form inter-particulate bonds of similar strength (Vromans, Deboer, Bolhuis, Lerk, Kussendrager, et al. 1985). With this approach, the differences in tabletability and compactibility between the powders are mechanistically explained by differences in microstructure and bonding area of the tablets, rather than by differences in bond strength. In the discussion (Section 4.3) of the physical significance of the rate parameters and their different dependencies on original particle diameter, the terms contact area and bonding area are used and the term proximity bonds introduced.

Furthermore, one should be aware of that both the compression and the compaction properties can be influenced by the rate at which the powder is compressed and compacted (Roberts and Rowe 1985). It is thus important to perform these experiments under precise and standardised conditions with a controlled punch travel pattern and velocity. For crystalline lactose, the deformation properties has been reported as strain rate sensitive (Roberts and Rowe 1985; Paul et al. 2019) whereas the tablet tensile strength was insensitive to strain rate (Paul et al. 2019).

4.1. Particle plastic stiffness

Crystalline lactose has been described as a brittle-ductile material (Hersey and Rees 1971), and it has been proposed that a brittle-ductile transition occurs for α-lactose monohydrate crystals at a particle size of 27.4 μm (Roberts and Rowe 1987). The Heckel equation is the most commonly used equation to assess the particle plastic stiffness of pharmaceutical materials and was used in this study. The Heckel approach has however received criticism in the literature (Rue and Rees 1978; Sonnergaard, 1999) and other relationships has been argued to be advantageous in terms of deriving an indication of the plastic properties of materials (Sonnergaard, 1999; Egart et al. 2014). However, the Heckel relationship has recently (Vreeman and Sun 2021) been proposed to be a reliable approach to quantify particle plastic stiffness. In this study a marked increase in plastic stiffness occurred at a particle size of about 20–30 μm, which hence is similar to the particle size reported for the ductile-brittle transition. In another study (Pazesh et al. 2017), it was found that ball milling of α-lactose monohydrate gave a minimum particle size of 5–6 μm, showing that fragmentation of small lactose particles is difficult to achieve. It is concluded that the coarser grades of the lactose powders used in this study can be described as predominantly brittle during compression and will show a high degree of fragmentation, while the finer grades can be described as predominantly plastic and show a limited degree of fragmentation during compression. This is consistent with an earlier observation (Alderborn and Nyström 1985) that a reduced original particle size decreased the relative degree of fragmentation that occurred during compression. However, since there was a distribution in particle size for the powders, it is possible that a fraction of particles of the finer grades of lactose powders fragmented during compression.

4.2. Experimental profiles vs models

The three-stage model of a tabletability profile gave reasonable approximations of the experimental profiles (Figure 5). However, two types of deviations from the model were obvious and obtained, in particular, for the finer grades of the lactose powders. First, two of the finest grades of lactose powders (LCMF and LH300) did not show a constant tablet strength at the highest compaction pressures; instead, it was a maximum strength followed by a small gradual decreased strength with increased applied pressure (Figure 5(f–g)). The absence of a stable plateau may be due to the formation of flaws or micro-cracks in tablets of very low porosity, flaws at which the fracture is initiated during strength testing and hence, reduces the fracture strength. It can be speculated that such flaws may be caused by the entrapment of air in the powder bed during die filling (Long and Alderton 1960). The entrapment of air may cause capping or lamination of tablets (Mazel et al. 2015), which typically are displayed as a reduced tensile strength and can thus explain the unstable plateau. Secondly, the three finest grades of the powders (LH230, LCMF and LH300) showed a more pronounced sigmoidal shape with an initial upward bending of the part of the

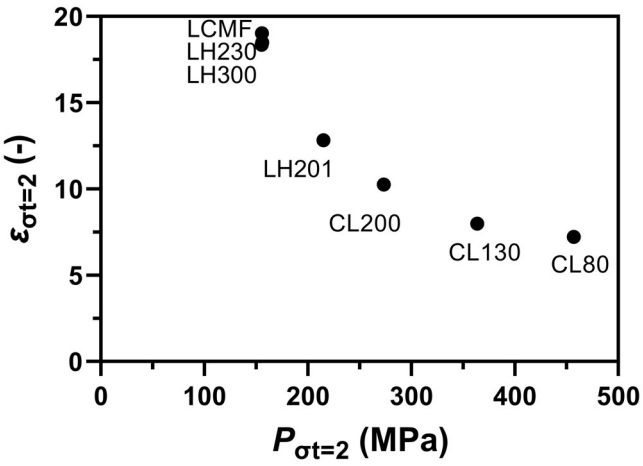

Figure 9. Porosity as a function of compaction pressure for a hypothetical tablet with a tensile strength of 2 MPa. The porosity $\varepsilon_{\sigma t=2}$ and the pressure ($P_{\sigma t=2}$) for the hypothetical tablet were calculated using the linear compactibility and tabletability relationships.

profile during which the tensile strength increased with compaction pressure (Figure 5(e,f)). Thus, the finest powders required a higher applied pressure to reach a consolidation state of the powder bed that subsequently resulted in an almost linear increase in tablet strength with compaction pressure. The finest lactose grades consist of very small particles (median particle diameters below 10 μm) that spontaneously form weak agglomerates of different size. The microstructure of the bed of powder in the die before compression is hence probably more heterogeneous than for powders of the coarser lactose grades that are less prone to forming such self-agglomerates. During the initial compression phase, it is likely that the agglomerates will break and fragment, parallel with a marked rearrangement of particles, and the microstructure will change markedly with pressure, manifested as an initial non-linear tensile strength-applied pressure relationship. After this initial phase, a more homogenous microstructure may be formed, and the rate of compression can thereafter be constant in the same fashion as the coarser grades. When a load is applied to a powder bed, it will be transmitted by a system of load bearing columns (Travers et al. 1987; Erikson et al. 2002). It can be speculated that a constant rate of compression is achieved when a certain quasi-static structure of such load-bearing columns is formed.

The Ryshkewitch–Duckworth model of a compactibility profile also gave reasonable approximations of the experimental profiles (Figure 6), but deviations from the model were evident for most powders. First, some powders gave slightly bended profiles, most clearly expressed at the higher tablet porosities. Secondly, some of the powders gave a levelling off at the lowest tablet porosities, which probably will affect the extrapolated tablet tensile strength. Consequently, σ_0 was determined by extrapolation in two ways due to this tendency of a deviation from linearity at low tablet porosities. For the coarser grades of powders, similar values of σ_0 were obtained in both cases, while for the finer grades the exclusion of some values at low tablet porosities gave higher values of σ_0 (Table 3). Thus, the choice of porosity range in the derivation of the Ryshkewitch–Duckworth parameters may affect the value of σ_0. An explanation for a levelling off of the Ryshkewitch–Duckworth plot at low tablet porosities, as proposed previously (Pazesh et al. 2019), is that there is a change in fracture part during strength testing, from around to across grain as dominating fracture path.

4.3. Physical significance of compaction parameters

4.3.1. Tabletability and compactibility endpoint parameters

The tabletability end-point parameter $\sigma_{t,\,max}$ is the maximum tensile strength that could be obtained during the loading situation used and represents the practical compaction endpoint. The compactibility end-point parameter σ_0 is a theoretical compaction endpoint typically determined by extrapolation.

Irrespective of the compaction pressure applied during compression, a consistent relationship between original particle diameter and tablet tensile strength was obtained (Figure 4). For the tablets of low tensile strength, it is reasonable that the interactions between the particles are weak, and the tablets fail at the inter-particulate junctions (around grain failure) while loaded. Thus, the particle-particle bonding will control the tablet strength. When the strength of tablets increases due to a reduced porosity, a change toward a more complicated fracture path with both around and across grain fracture may occur. The tablet strength may then be controlled by the combination of the strength of the particles and the sum of the strength of the bonds holding the particles together. However, here it is argued that since the relationship between tablet tensile strength and original particle diameter is preserved with reduced tablet porosity, the inter-particulate bonds will also control the tensile strength for the tablets prepared at the highest compaction pressures. The $\sigma_{t,\,max}$ is thus physically explained by the total strength of the inter-particulate bonds at the fracture plane.

The physical meaning of σ_0 is less obvious, and it may be understood in different ways (Pazesh et al. 2019), i.e. as an intrinsic strength of the material, independent of particle size, the strength of the particles forming the compact or the strength of the bonds between the particles. For the parameter to be an intrinsic property, it is required that the compaction of various size qualities of a given material eventually forms a nonporous solid unit. In this study, it is found (Table 3) that the original particle diameter markedly affected the σ_0, which is consistent with an earlier report (Adolfsson and Nyström 1996). Thus, the effect of particle size is not eliminated by the extrapolation, and it is concluded that σ_0 does not represent an intrinsic material property. It is also reported that the value is affected by the loading situation, such as the compaction speed (Steendam and Lerk 1998), supporting that the value cannot correspond to an intrinsic strength of the material. Also, for σ_0, the same relationship between original particle diameter and tablet tensile strength was obtained as for the tablets, for which the tensile strength was measured (Figure 4), also shown by the nearly constant ratio of 2–3 between σ_0 and the $\sigma_{t,\,max}$ (Table 3). Thus, both σ_0 and $\sigma_{t,\,max}$ reflect essentially the same property of the compacted specimen and are thus controlled by the same microstructural feature of the tablet. It is hence proposed that for the powders used in this study, σ_0 is physically explained as an indication of the total strength of the inter-particulate bonds at the fracture plane. This conclusion is consistent with an earlier proposal (Pazesh et al. 2019) that σ_0 is an indication of the total strength of the inter-particulate bonds over the tablet cross-section for tablets that obey the Ryshkewitch–Duckworth equation approximately. However, under certain circumstances, the strength of the inter-particulate bond network approaches the particle strength, and the latter may then control $\sigma_{t,\,max}$ and σ_0, instead. We have previously referred to these two circumstances (Pazesh et al. 2019) as typical and atypical compaction behaviour, respectively.

Another indication of the effect of particle size on the tabletability and compactibility of the lactose powders is to use the linear regression equations for the tabletability and compactibility

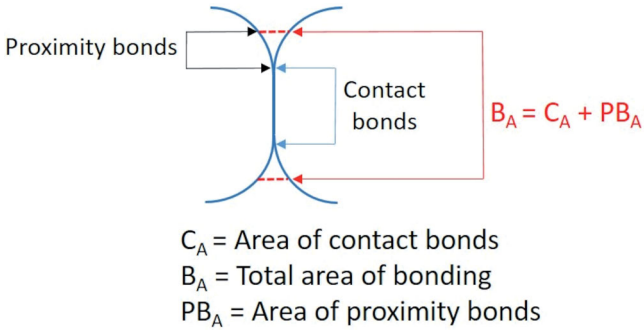

Figure 10. Illustration of bonding conception.

profiles to calculate the compaction pressure and the porosity needed to obtain a tablet tensile strength of 2 MPa (as is a common value of tablet tensile strength during tablet manufacturing (Leane et al. 2015)). A compaction pressure of about 150 MPa and a porosity of 18% were needed to reach the target tensile strength for LH230, LCMF and LH300 ($d_{50} < 10\,\mu m$; Figure 9), whereas for the larger powders, increasing pressure in combination with a reduced porosity is needed to reach the same target tensile strength.

4.3.2. Tabletability and compactibility rate parameters

It has previously been proposed (Alderborn 2003) that the gradient of the linear part of a tabletability profile is controlled by the increase in inter-particulate contact area per pressure unit, i.e. the evolution in tensile strength is directly proportional to the increase in contact area. The concept is based on a microstructural evolution of the tablet, focused on the process occurring at the inter-particulate junctions. The contact area is assumed to be controlled by the degree of deformation, which is dependent on the hardness or plastic stiffness of the particles and the applied contact force. This conception is consistent with a linear increase in tablet strength with pressure until a finite contact area is reached. The obtained experimental tabletability profiles (Figure 5) approximately obey this theoretical relationship. It was also proposed (Alderborn 2003) that the pressure range within which the tensile strength depends on the applied pressure in a linear way is proportional to the yield pressure. Since the yield pressures (Table 2) were similar between the powders, it is to be expected that there is a correlation between the slope of the linear part and the maximum tensile strength, which was also the case (Figure 8(a)). This relationship also has a defined starting point at the origin of the axes, i.e. if it is not possible to form a tablet irrespective of applied pressure, there will not be any region within which the tablet strength will increase. A linear regression of the $\sigma_{t,\,max}$ vs k_c plot gave however an extrapolated intercept, which was somewhat higher than zero, i.e. 1.16 MPa.

According to the derivation of the three-stage model, the gradient of the linear part of the profile should be independent of the original size of the particles. This was obviously not the case for the powders used in this study. The inter-particulate contact area, or area of contact bonds, is defined here as the area of contact developed during powder compression between a pair of particles due to particle plastic deformation. The bonding area can be defined as the total area of attractive bonds acting between a pair of particles. Inter-molecular bonding forces act over some distance, and a close packing of particles may hence provide the condition for a fraction of the particle surface area to take part in particle–particle bonding in direct vicinity to the area of contact. Such attractive forces are referred to here as proximity bonds. The bonding area is then the sum of contact area (area of contact bonds) and the area of proximity bonds, illustrated in Figure 10. Depending on the microstructure of the compact, the bonding area to contact area ratio may differ between compacts. Since small particles are more closely packed in tablets with inter-particulate pores of lower diameter, small particles will have a larger bonding area to contact area ratio than larger particles. This conception can explain the particle size dependent difference in slope of the tabletability profiles.

The rate constant k_R of the Ryshkewitch–Duckworth equation has been denoted a bonding capacity factor (Steendam and Lerk 1998), a term indicating that the slope should reflect some ability of the powder to bind due to the application of pressure. This will probably mean that a high k_R should be related to a high σ_0. The slopes of the compactibility profiles showed however a small variation compared to the slopes of the tabletability profiles. Moreover, rather than having a similar point of origin, as was the case for the tabletability profiles which all originated close to the origin of the axes, the profiles were shifted along the strength axis in an almost parallel manner (Figure 6(h)). The compactibility of the powders were thus described predominantly by the position of the profiles along the tablet strength axis rather than by the slope of the profiles, and these positions controlled the extrapolated σ_0. It has also been reported previously (Wu et al. 2006; Mishra and Rohera 2019) that an increased σ_0 may not correspond to an increased k_R, which is consistent with the results in this paper (Table 3), i.e. a powder may generally compact into tablets of high tensile strength without having a marked change in tensile strength due to increased solid fraction (Wu et al. 2006).

Tablet porosity is a global tablet property and not based directly on an analysis of the contact process occurring between particles in the compact. However, the tablet porosity is an indication of the microstructure of the tablet, and it is to be expected that a decreased porosity will typically correspond to a more closed pore system due to fragmentation and deformation of the particles and hence also an increased area of contact between the particles. The similar dependency of the tablet porosity for all the lactose powders indicates that the evolution in tensile strength is controlled by the same microstructural feature of the tablet, independent of the original particle size. This character of the compactibility profiles can be explained using the same conception as used to explain the different slopes of the tabletability profiles, i.e. by an increased bonding area – contact area ratio with decreased original particle size due to larger areas of proximity bonds. Accordingly, the constant k_R reflects the evolution in contact area with decreased tablet porosity, which was similar between the powders and hence, almost independent of particle size. Moreover, the changed position along the tablet strength axis reflects a particle size dependent change in bonding area – contact area ratio.

Although the k_R varied only slightly between the powders, one may note that if compactibility profiles are grouped, depending on the brittle-plastic transition diameter, two sub-groups can be distinguished as indicated in Figure 8(b), where one sub-group constitutes of CL80, CL130, CL200 and LH201 and the other sub-group of LH230, LCMF and LH300. Within each sub-group, a small increase in slope k_R was obtained with increased σ_0. Thus, it seems that the evolution in microstructure showed some dependency of original particle size, i.e. an increased σ_0 corresponded to a slight increase in k_R within each group of powders. Since the powders in each sub-group can be argued to have different mechanical properties, i.e. are predominantly brittle or predominantly plastic, it is possible that the k_R was also affected by the

degree of fragmentation that is expressed during compaction of these α-lactose monohydrate powders.

5. Conclusions

This paper reports on the tabletability and the compactibility of a series α-lactose monohydrate powders, ranging in particle size from approximately 3.5 to 203 μm. The main proposed findings of the study are the following:

- The original median particle diameter generally had a strong effect on the tablet tensile strength and thus also on the tabletability and compactibility profiles. The experimental profiles were reasonably approximated using the three-stage compaction model and using the Ryshkewitch–Duckworth compaction equation, and the compaction parameters derived were hence regarded as representative of the experimental profiles.
- The two compaction endpoint parameters, i.e. σ_0 and $\sigma_{t,max}$, increased with decreased particle size and were both controlled by the total strength of the inter-particulate bonds acting over the tablet cross-section.
- The tabletability rate parameter k_c increased with decreased particle size and correlated well with the tabletability endpoint parameter and is controlled by the evolution in inter-particulate bond network. In addition, the tabletability rate parameter k_c was also markedly affected by a particle size dependent ratio between bonding area and contact area, i.e. this ratio increased with a reduced particle size.
- The compactibility rate parameter k_R tended to increase with decreased particle size but the effect was limited, and no correlation between the compactibility rate and endpoint parameters was obtained. The compactibility rate parameter k_R reflects the evolution in contact area with decreased tablet porosity, and the changed position of the strength-porosity plots along the tablet strength axis reflects a particle size dependent change in bonding area – contact area ratio. Moreover, this parameter may be affected by the particle size through a brittle-plastic transition.

In conclusion, the compactibility and tabletability analysis provides supplementary information of the compact forming ability of a powder; collectively, these parameters give collectively a concentrated description of the compaction properties of a powder It is believed that these findings are applicable to tablets of other crystalline powders showing similar fracture propagation mechanism during strength testing as the α-lactose monohydrate powders used in this study. However, tablets formed of more complex materials, e.g. disordered materials, may have a different fracture propagation mechanism during testing which may affect the tabletability and compactibility profiles and hence the derived parameters. In a follow-up study, we intend to investigate the possibility of using a hybrid approach to predict the tabletability and compactibilty of these lactose powders.

Acknowledgements

The authors wish to thank Bakhita Idris (MSc) for experimental assistance in analysis of CL130, LH200 and LH300, and Lucia Lazorova (PhD) for capturing the SEM images.

Disclosure statement

The authors report no competing interest.

Funding

The author(s) reported there is no funding associated with the work featured in this article.

Author contributions

Ann-Sofie Persson: Conceptualisation, Methodology, Validation, Investigation, Writing – Original Draft. Samaneh Pazesh: Methodology, Investigation, Writing – Review and editing. Göran Alderborn: Conceptualisation, Methodology, Writing – Review and editing, Supervision, Resources, Funding acquisition, Project administration.

References

Adolfsson A, Nyström C. 1996. Tablet strength, porosity, elasticity and solid state structure of tablets compressed at high loads. Int J Pharm. 132(1–2):95–106.

Alderborn G. 2003. A novel approach to derive a compression parameter indicating effective particle deformability. Pharm Dev Technol. 8(4):367–377.

Alderborn G, Börjesson E, Glazer M, Nyström C. 1988. Studies on direct compression of tablets XIX. The effect of particle size and shape on the mechanical strength of sodium bicarbonate tablets. Acta Pharm Suec. 25(1):31–40.

Alderborn G, Nyström C. 1982. Studies on direct compression of tablets IV. The effect of particle size on the mechanical strength of tablets. Acta Pharm Suec. 19(5):381–390.

Alderborn G, Nyström C. 1985. Studies on direct compression of tablets XIV. The effect of powder fineness on the relation between tablet permeametry surface area and compaction pressure. Powder Technol. 44(1):37–42.

Butcher AE, Newton JM, Fell JT. 1974. Tensile failure planes of powder compacts. Powder Technol. 9(1):57–59.

Cabiscol R, Shi H, Wünsch I, Magnanimo V, Finke JH, Luding S, Kwade A. 2020. Effect of particle size on powder compaction and tablet strength using limestone. Adv Powder Technol. 31(3):1280–1289.

Castellanos A. 2005. The relationship between attractive interparticle forces and bulk behaviour in dry and uncharged fine powders. Adv Phys. 54(4):263–376.

Chang S-Y, Wang C, Sun CC. 2019. Relationship between hydrate stability and accuracy of true density measured by helium pycnometry. Int J Pharm. 567:118444.

Duckworth W. 1953. Discussion of Ryshkewitch paper. J Am Ceram Soc. 36:68.

Egart M, Ilic I, Jankovic B, Lah N, Srcic S. 2014. Compaction properties of crystalline pharmaceutical ingredients according to the Walker model and nanomechanical attributes. Int J Pharm. 472(1–2):347–355.

Erikson JM, Mueggenburg NW, Jaeger HM, Nagel SR. 2002. Force distributions in three-dimensional compressible granular packs. Phys Rev E. 66(4 Pt 1):040301.

Fell JT, Newton JM. 1970. Determination of tablet strength by the diametral-compression test. J Pharm Sci. 59(5):688–691.

Fichtner F, Mahlin D, Welch K, Gaisford S, Alderborn G. 2008. Effect of surface energy on powder compactibility. Pharm Res. 25(12):2750–2759.

Heckel RW. 1961. Density-pressure relationships in powder compaction. T Metall Soc AIME. 221(4):671–675.

Hersey JA, Rees JE. 1971. Deformation of Particles during Briquetting. Nat Phys Sci. 230(12):96–96.

Hersey JA, Rees JE, Cole ET. 1973. Density changes in lactose tablets. J Pharm Sci. 62(12):2060.

Ilic I, Kasa P, Dreu R, Pintye-Hodi K, Srcic S. 2009. The compressibility and compactibility of different types of lactose. Drug Dev Ind Pharm. 35(10):1271–1280.

Kawakita K, Lüdde K-H. 1971. Some considerations on powder compression equations. Powder Technol. 4(2):61–68.

Knudsen FP. 1959. Dependence of mechanical strength of brittle polycrystalline specimens on porosity and grain size. J Am Ceram Soc. 42(8):376–387.

Kuentz M, Leuenberger H. 2000. A new theoretical approach to tablet strength of a binary mixture consisting of a well and a poorly compactable substance. Eur J Pharm Biopharm. 49(2): 151–159.

Leane M, Pitt K, Reynolds G, Manufacturing Classification System (MCS) Working Group. 2015. A proposal for a drug product Manufacturing Classification System (MCS) for oral solid dosage forms. Pharm Dev Technol. 20(1):12–21.

Long WM, Alderton JR. 1960. The displacement of gas from powders during compaction. Powder Metall. 3(6):52–72.

Mahmoodi F, Klevan I, Nordström J, Alderborn G, Frenning G. 2013. A comparison between two powder compaction parameters of plasticity: the effective medium A parameter and the Heckel 1/K parameter. Int J Pharm. 453(2):295–299.

Mazel V, Busignies V, Diarra H, Tchoreloff P. 2015. Lamination of pharmaceutical tablets due to air entrapment: direct visualization and influence of the compact thickness. Int J Pharm. 478(2):702–704.

Mishra SM, Rohera BD. 2019. Mechanics of tablet formation: a comparative evaluation of percolation theory with classical concepts. Pharm Dev Technol. 24(8):954–966.

Newton JM, Rowley G, Fell JT, Peacock DG, Ridgway K. 1971. Computer analysis of relation between tablet strength and compaction pressure. J Pharm Pharmacol. 23:S195–S201.

Nordström J, Klevan I, Alderborn G. 2009. A Particle Rearrangement Index Based on the Kawakita Powder Compression Equation. J Pharm Sci. 98(3):1053–1063.

Nordström J, Welch K, Frenning G, Alderborn G. 2008. On the physical interpretation of the Kawakita and Adams parameters derived from confined compression of granular solids. Powder Technol. 182(3):424–435.

Orowan E. 1949. Fracture and strength of solids. Rep Prog Phys. 12(1):185–232.

Paul S, Tajarobi P, Boissier C, Sun CC. 2019. Tableting performance of various mannitol and lactose grades assessed by compaction simulation and chemometrical analysis. Int J Pharm. 566:24–31.

Pazesh S, Gråsjö J, Berggren J, Alderborn G. 2017. Comminution-amorphisation relationships during ball milling of lactose at different milling conditions. Int J Pharm. 528(1-2):215–227.

Pazesh S, Persson A-S, Alderborn G. 2019. Atypical compaction behaviour of disordered lactose explained by a shift in type of compact fracture pattern. Int J Pharm X. 1:100037.

Pazesh S, Persson A-S, Berggren J, Alderborn G. 2018. Effect of milling on the plastic and the elastic stiffness of lactose particles. Eur J Pharm Sci. 114:138–145.

Persson A-S, Ahmed H, Velaga SP, Alderborn G. 2018. Powder compression properties of paracetamol, paracetamol hydrochloride, and paracetamol cocrystals and coformers. J Pharm Sci. 107(7):1920–1927.

Persson A-S, Alderborn G. 2018. A hybrid approach to predict the relationship between tablet tensile strength and compaction pressure using analytical powder compression. Eur J Pharm Biopharm. 125:28–37.

Rees JE, Rue PJ. 1978. Work required to cause failure of tablets in diametral compression. Drug Dev Ind Pharm. 4(2):131–156.

Roberts RJ, Rowe RC. 1985. The effect of punch velocity on the compaction of a variety of materials. J Pharm Pharmacol. 37(6): 377–384.

Roberts RJ, Rowe RC. 1987. Brittle/ductile behaviour in pharmaceutical materials used in tabletting. Int J Pharm. 36(2-3): 205–209.

Rue PJ, Rees JE. 1978. Limitations of the Heckel relation for predicting powder compaction mechanisms. J Pharm Pharmacol. 30(10):642–643.

Ryshkewitch E. 1953. Compression strength of porous sintered alumina and zirconia. J Am Ceram Soc. (2)36:65–68.

Sonnergaard JM. 1999. A critical evaluation of the Heckel equation. Int J Pharm. 193(1):63–71.

Sonnergaard JM. 2006. Quantification of the compactibility of pharmaceutical powders. Eur J Pharm Biopharm. 63(3):270–277.

Steendam R, Lerk CF. 1998. Poly(dl-lactic acid) as a direct compression excipient in controlled release tablets: Part I. Compaction behaviour and release characteristics of poly(dl-lactic acid) matrix tablets. Int J Pharm. 175(1):33–46.

Sun C. 2004. A novel method for deriving true density of pharmaceutical solids including hydrates and water-containing powders. J Pharm Sci. 93(3):646–653.

Travers T, Ammi M, Bideau D, Gervois A, Messager JC, Troadec JP. 1987. Uniaxial compression of 2d packings of cylinders. Effects of weak disorder. Europhys Lett. 4(3):329–332.

Tye CK, Sun CC, Amidon GE. 2005. Evaluation of the effects of tableting speed on the relationships between compaction pressure, tablet tensile strength, and tablet solid fraction. J Pharm Sci. 94(3):465–472.

Vreeman G, Sun CC. 2021. Mean yield pressure from the in-die Heckel analysis is a reliable plasticity parameter. Int J Pharm X. 3:100094.

Vromans H, Deboer AH, Bolhuis GK, Lerk CF, Kussendrager KD. 1985. Studies on tabletting properties of lactose. Part 1. The effect of initial particle-size on binding properties and dehydration characteristics of lactose. Acta Pharm Suec. 22(3):163–172.

Vromans H, De Boer AH, Bolhuis GK, Lerk CF, Kussendrager KD, Bosch H. 1985. Studies on tableting properties of lactose. Part 2. Consolidation and compaction of different types of crystalline lactose. Pharm Weekbl Sci. 7(5):186–193.

Wu CY, Best SM, Bentham AC, Hancock BC, Bonfield W. 2005. A simple predictive model for the tensile strength of binary tablets. Eur J Pharm Sci. 25(2-3):331–336.

Wu CY, Best SM, Bentham AC, Hancock BC, Bonfield W. 2006. Predicting the tensile strength of compacted multi-component mixtures of pharmaceutical powders. Pharm Res. 23(8): 1898–1905.